HHS Public Access

Author manuscript

J Allergy Clin Immunol. Author manuscript; available in PMC 2022 September 01.

Published in final edited form as:

J Allergy Clin Immunol. 2021 September ; 148(3): 799–812.e10. doi:10.1016/j.jaci.2021.02.018.

Basophils promote barrier dysfunction and resolution in the atopic skin

Christophe Pellefigues, PhD[a,b], **Karmella Naidoo, PhD**[a,*], **Palak Mehta, MS**[a,*], **Alfonso J. Schmidt, MS**[a,*], **Ferdinand Jagot, MS**[a], **Elsa Roussel, MS**[c], **Alissa Cait, PhD**[a], **Bibek Yumnam, MS**[a], **Sally Chappell, MS**[a], **Kimberley Meijlink, MS**[a], **Mali Camberis, MS**[a], **Jean X. Jiang, PhD**[d], **Gavin Painter, PhD**[e], **Kara Filbey, PhD**[a], **Özge Uluçkan, PhD**[c], **Olivier Gasser, PhD**[a], **Graham Le Gros, PhD**[a]

[a]Malaghan Institute of Medical Research, Victoria University, Wellington, New Zealand;

[b]INSERM UMR1149, CNRS ERL8252, Centre de recherche sur l'inflammation, Inflamex, Université de Paris;

[c]Novartis Institutes for Biomedical Research (NIBR), Novartis, Basel;

[d]Department of Biochemistry and Structural Biology, University of Texas Health Science Center, San Antonio;

[e]Ferrier Research Institute, Victoria University, Wellington.

Abstract

Background: The type 2 cytokines IL-4 and IL-13 promote not only atopic dermatitis (AD) but also the resolution of inflammation. How type 2 cytokines participate in the resolution of AD is poorly known.

Objective: Our aim was to determine the mechanisms and cell types governing skin inflammation, barrier dysfunction, and resolution of inflammation in a model of AD.

Methods: Mice that exhibit expression of IL-4, IL-13, and MCPT8 or that could be depleted of basophils or eosinophils, be deficient in IL-4 or MHC class II molecules, or have basophils lacking macrophage colony-stimulating factor (M-CSF) were treated with calcipotriol (MC903) as an acute model of AD. Kinetics of the disease; keratinocyte differentiation; and leukocyte accumulation, phenotype, function, and cytokine production were measured by transepidermal water loss, histopathology, molecular biology, or unbiased analysis of spectral flow cytometry.

Results: In this model of AD, basophils were activated systemically and were the initial and main source of IL-4 in the skin. Basophils and IL-4 promoted epidermal hyperplasia and skin barrier dysfunction by acting on keratinocyte differentiation during inflammation. Basophils, IL-4, and basophil-derived M-CSF inhibited the accumulation of proinflammatory cells in the

Corresponding author: Christophe Pellefigues, PhD, Centre de recherche sur l'inflammation, INSERM UMR1149, CNRS ERL8252, Université de Paris, Paris 75018, France. Christophe.pellefigues@inserm.fr.

*These authors contributed equally to this work.

Disclosure of potential conflict of interest: The authors declare that they have no relevant conflicts of interest.

skin while promoting the expansion and function of proresolution M2-like macrophages and the expression of probarrier genes. Basophils kept their proresolution properties during AD resolution.

Conclusion: Basophils can display both beneficial and detrimental type 2 functions simultaneously during atopic inflammation.

GRAPHICAL ABSTRACT

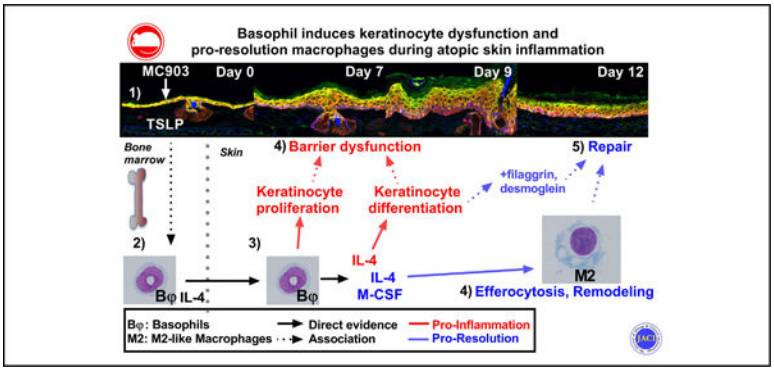

Keywords

Atopic dermatitis; basophils; M2; macrophages; efferocytosis; type 2 inflammation; resolution; IL-4; M-CSF

Atopic dermatitis (AD) is the most common chronic skin condition, affecting up to 20% of the population. It is characterized by intense itch episodes and epidermal barrier dysfunction that is associated both epidemiologically and, in mice models, with the release of thymic stromal lymphopoietin (TSLP), IL-33, IL-4, IL-13, and histamine.[1] TSLP and IL-33 can be secreted by the inflamed epidermis to directly induce the secretion of IL-4/13 by type 2 innate cells.[2,3] The efficacy of dupilumab (a mAb targeting IL-4Rα) in AD underlines the critical functional role of IL-4 and/or IL-13 in this pathology.[4]

Type 2 cytokines and histamine act on keratinocytes to prevent their timely differentiation in an ordered epidermis.[5] Alongside TSLP, they also promote chronic itch through direct effects on sensory neurons.[6] Keratinocyte differentiation and itch-scratch cycles are critical contributors to the epidermal hyperplasia and barrier dysfunction observed in AD.[1,4] This leaky barrier enables the establishment of chronic inflammation and skin dysbiosis, and it allows entry of allergens that promote development of the atopic march.[7]

Basophils are rare circulating granulocytes that can secrete type 2 cytokines and histamine.[8] They exacerbate T_H2 cell differentiation,[9] and they infiltrate the skin to activate type 2 innate lymphoid cell (ILC2) expansion and IL-13 secretion in AD-like disease through their secretion of IL-4.[10,11] Basophils have been considered both proinflammatory[10,12] and anti-inflammatory.[13] Indeed, they infiltrate the dermis in diverse skin conditions[14] to induce epidermal hyperplasia[15,16] or support the resolution of inflammation.[16–18]

Besides their pathogenic role in atopic diseases, type 2 cytokines are involved in tissue remodeling and resolution by inducing a M2 macrophage phenotype.[19] M2-

like macrophages contain heterogeneous subsets specialized in efferocytosis, resolution of inflammation, repair, and remodeling.[20–22] The dermis contains several subsets of macrophages, including $CD64^+$ MHC class II–high ($MCHII^{hi}$) monocyte–derived macrophages and $CD64^+CD206^{hi}$ dermal-resident self-renewed macrophages.[23,24] The expression of CD206 by macrophages is induced by type 2 cytokines and is critical for the resolution of inflammation and tissue remodeling through proinflammatory molecule scavenging and the phagocytosis of collagen fibers, respectively.[25,26]

We used an established model of AD initiated by the topical application of calcipotriol (MC903) on the ear for 4 days,[27] which is known to be dependent on epidermal TSLP expression.[28] This led to an acute AD-like inflammation peaking at days 9 and 10, followed by a spontaneous resolution. Unbiased high-dimensional spectral flow cytometry analysis revealed that basophils were the main source of IL-4 in the skin during both inflammation and its resolution. Basophil depletion, or genetic deletion of IL-4, were sufficient to delay and reduce epidermal hyperplasia and barrier dysfunction. Basophils also induced the expansion of M2 macrophages, efferocytosis, and probarrier genes, which are key indicators of the resolution phase. Thus, basophils play both pathogenic and prohomeostatic roles in a mouse model of AD.

METHODS

Mice

Six- to 12-week-old, Basoph8 (B8) mice (which express the Cre recombinase and the eYFP under the control of MCPT8, specifically in basophils),[29,30] Cre-inducible diphtheria toxin receptor (iDTR) mice (expressing the simian diphtheria toxin receptor upon Cre activity),[31] and dsRed.T3 (dsRed, ubiquitous expression) were obtained from Jackson Laboratory. C57BL/6J mice were obtained from Jackson Laboratory or Charles River Germany, iPhil mice (which express the simian DTR specifically in eosinophils) were obtained from James J. Lee (Mayo Clinic Arizona),[32] $IL\text{-}4^{G4/G4}$ (IL-4KO) mice (which express the green fluorescent protein as a knockin, inactivating IL-4 expression)[33] and 4C13R mice (dual reporter of IL-4 and IL-13 expression)[30,34] were obtained from Bill Paul (National Institutes of Health [NIH]), $CSF1^{fl/fl}$ mice were obtained from Dr Jean X. Jiang (San Antonio University),[35] TSLPRKO mice[36] were obtained from Dr Warren Leonard (NIH), and MHCIIKO mice were gifted by Dr Horst Bluethmann (Hoffman-La Roche, Basel, Switzerland).[37] All mice were bred, crossed, and housed in specific pathogen–free conditions at the Malaghan Institute of Medical Research Biomedical Research Unit or Novartis Institute for Biomedical Research Center. All experimental protocols were approved by the Victoria University of Wellington Animal Ethics Committee (permit 24432) and performed according to local institutional guidelines. Unless specified, only female mice were used, as leukocytes and type 2 cytokine expression showed different kinetics in our models (data not shown). Littermates were used for all experiments comparing groups issued from parents with the same genotype.

Treatments

The mice were anaesthetized by intraperitoneal injection of ketamine/xylazine, and 4 nmol of MC903 (Calcipotriol, Cayman Chemicals, Ann Arbor, Mich) in 100% ethyl alcohol (EtOH) was applied topically daily for 4 days in 20 μL (10 μL per side), whereas EtOH was applied on the contralateral ear. Diphtheria toxin (Cayman Chemicals) was injected intraperitoneally in the amount of 20 ng/g per day into B8×iDTR mice and every 2 days into iPhil mice.[30,38] AM156 or vehicle was delivered intragastrically daily from day −1 to day 3 (250 μL, 1 mg/mL in 0.5% methylcellulose) as described.[38] Apoptosis of dsRed mice splenocytes was induced in Iscove modified Dulbecco medium with 10% FCS (Gibco, ThermoFischer, Watham, Mass) plus 1 μM dexamethasone at a concentration of 10^6/mL for 24 hours at 37°C and 5% CO_2 (>90%) and then washed 3 times in excess PBS before being resuspended at 100 × 10^6/mL. Next, 20 μL of apoptotic cells was injected intradermally for efferocytosis analysis. One mg of neutralizing anti-mouse IL-4 (Novartis Institutes for Biomedical Research, Switzerland) or rat IgG1 isotype were injected intraperitoneally every other day for IL-4 neutralization experiments.

Measurements, histology, and microscopy

Ear thickness and transepidermal water loss (TEWL) were measured on sedated mice with a digital caliper (Kroeplin, Germany) and the DERMALAB TEWL probe (Cortex Technology, Denmark)[38] or Tewameter TM Nano (Courage + Khazaka Electronics, Japan). Serum IgE was quantified by using a mouse IgE ELISA kit (Mybiosource.com, San Diego, Calif; catalog no. MBS564074). Ear tissue was fixed in 4% paraformaldehyde for 24 hours, processed, paraffin-embedded, sectioned at 4 μm, and stained with hematoxylin and eosin to measure epidermal and dermal thickness or with Masson trichrome (Millipore-Sigma, Burlington, Mass) to measure the area of collagen as the percentage of the blue area from the total ear area by using ImageJ software (NIH). Images were viewed on a widefield Olympus brightfield microscope (BX51) with a 20× NA 0.5 objective and cellSens software (Olympus, Japan). For immunofluorescence, whole ears were incubated for 1 hour at 4°C in 20% sucrose; rinsed; snap-frozen in OCT compound in liquid nitrogen; sectioned at 8 μm; blocked in Superblock (ThermoFisher); and stained with rabbit antifilaggrin (Poly19058), chicken antikeratin 14 (anti-K14) (Poly9060), rat anti–Ki-67 (16A8, both from Biolegend, San Diego, Calif), and guinea pig antikeratin (anti-K10 [Progen, Germany]) overnight at 4°C. The sections were washed and stained with goat anti-rabbit IgG AF488 (catalog no. A27034, ThermoFisher), goat anti-chicken IgY AF647 (catalog no. Ab150171, Abcam, United Kingdom), and anti–guinea pig AF568 (catalog no. ab175714, Abcam) for 2 hours at 4°C before being washed and mounted for confocal analysis.[39] For the TUNEL assay, the Click-IT Plus TUNEL assay AF647 kit (ThermoFisher) was used as per the manufacturer's guidelines, alongside 4',6-diamino-2-phenylindole. Images were recorded on an IX83 inverted microscope equipped with a FV1200 confocal head by using a 20×, numeric aperture 0.75 objective and FV10-ASW, version 4.2b, software (Olympus) and then analyzed with ImageJ software (version 1.52n, NIH) or Cellprofiler software (version 3.1.8, Broad Institute, Cambridge, Mass).

Tissue digestion

Blood was collected by cheek bleeding or intracardial puncture. Red blood cells, bone marrow (BM) cells, and spleen cells were lysed in an ammonium chloride buffer and prepared as already described.[40] For the skin cell preparations, ears were split into the dorsal and ventral layers, minced, and digested for 30 minutes at 37°C in a shaking incubator (150 rpm) in Iscove modified Dulbecco medium with 5% FCS (Gibco, ThermoFischer) containing 2 mg/mL of collagenase IV and 100 μg/mL of DNAse I (Sigma-Millipore). Digestion was stopped by adding 5 mM EDTA and the tissue was filtered through a 70-μm nylon mesh filter (BD Biosciences, Franklin Lakes, NJ). For some experiments, ears were digested by using 0.25mg/mL of Liberase TM (Roche, Switzerland) for 20 minutes at 37°C and dissociated with a GentleMACS dissociator (Miltenyi, Germany).

Flow cytometry

Single-cell suspensions were blocked for 15 minutes at 4°C in fluorescence-activated cell sorting (FACS) buffer (1× PBS with 1% bovine serum albumin and 0.05% NaN_3 [Sigma]) containing 0.5% of 2.4G2 hybridoma supernatant. The cells were then stained in FACS buffer for 20 minutes at 4°C with an optimized panel of fluorophore-conjugated antibodies, unless otherwise specified. The antibodies used are presented in Table E1 (in the Online Repository at www.jacionline.org). A summary of gating strategies, which were previously described, is presented in Table E2 (in the Online Repository at www.jacionline.org).[41] Compensation was performed by using UltraComp eBeads (Invitrogen, ThermoFischer) as single stained positive controls or dsRed or B8 splenocytes; fluorescence minus 1 (FMO) controls were used to set background expression when needed. B8×C57 mice were used to set B8×4C13R positivity gates at FMO. Flow cytometry was performed on an Aurora spectral cytometer with 3 lasers (Cytek Biosciences, Fremont, Calif) or a Fortessa X20 (BD). FACS sorting was carried out on a BD Influx cell sorter (BD). T-distributed stochastic neighbor embedding analyses were done as Opt-SNE on default settings from at least 4 concatenated samples per group with use of FlowJo version X (BD).

Molecular biology

For cell-specific gene expression, 2,000 or 10,000 sort-purified cells were collected in RNA lysis buffer, and RNA was extracted by using a Quick-RNA kit (Zymo Research, Irvine, Calif). For whole skin gene expression, ears were snap-frozen, minced, homogenized by using 5-mm stainless steel beads and a Tissue Lyzer II (Qiagen, Germany), and RNA was extracted by using Trizol (ThermoFisher) and the Quick RNA kit (Zymo Research). cDNA was synthetized by using the High-Capacity RNA-to-cDNA kit (Applied Biosystems, ThermoFischer). Reverse-transcriptase quantitative PCR was performed with a QuantStudio 7 (Applied Biosystems) and following the manufacturer's guidelines, with use of SYBR Green Master Mix and the following probes (for *Gapdh*, forward 5'-AATGGTGAAGGTCGGTGTGA and reverse 5'-GCAACAATCTCCACTTTGCCA; for *Furin*, forward 5'-ACACACAGATGAATGACAAC and reverse 5'-GCATTGTAAGCTACACCTAC; and for *Dsg1*, forward 5'-AAGGCAGAAACGAGAATGGA and reverse 5'-CGAGATGCGGTATGTCACTG) or Taqman Master Mix (all from ThermoFisher) as a duplex with the probes described in

Table E3 (in the Online Repository at www.jacionline.org). Transcript levels were expressed as the ratio of $2^{-\Delta CT}$ to glyceraldehyde-3-phosphate dehydrogenase.

Statistics

Statistical analyses were performed by using Prism 8 or Prism 9 software (GraphPad Software Inc, La Jolla, Calif). Data from experimental replicates were pooled if doing so led to a decreased variance; alternatively, representative results from an individual experiment were represented. Parametric or nonparametric tests were used depending on the normality of the data distribution assessed with a D'Agostino-Pearson K2 omnibus test. Individual dots and/or means ± SEMs or median and the interquartile range or violin plots are shown, depending on the distribution. Posttest-adjusted *P* values are always represented when used. In all cases, *n* represents an individual mouse and a 2-tailed *P* value less than .05 was considered the threshold for significance.

RESULTS

MC903 induces an AD-like resolving epidermal pathology

After 4 days of daily MC903 treatment,[27] ear thickness and TEWL (a measure of epidermal dysfunction) continued to increase until day 9 or 10 before resolving, thus defining an inflammation phase (days 0–9) and a resolution phase (days 10–14) (Fig 1, A). Skin presentation included redness, stiffness, shrinking, dryness, progressive scaling of the skin of the ear (Fig 1, B). Although disease progression was associated with dermal and epidermal thickening (Fig 1, C), only epidermal swelling was associated with disease kinetics (Fig 1, D). The quantity of collagen in the dermis dropped during inflammation, before increasing during the resolution phase (Fig 1, E and F). A basal layer of $K10^{-}K14^{+}$ cells (stratum basale [Fig 1, G and H]) and a suprabasal layer of $K10^{-}K14^{+}$ keratinocytes (stratum spinosum [Fig 1, G and I]) expanded in the epidermis. $Ki67^{+}$ proliferating keratinocytes were found mostly in the stratum basale (Fig 1, J). The expression of profilaggrin (*Flg*), and an outer layer of fillagrin (FLG)-positive keratinocytes (stratum granulosum) expanded over time, exhibiting a peak of acanthosis at day 9.[42] Hyperkeratosis was evident from day 7 (Fig 1 C, E, and G). These features were observed alongside intercellular edemas (mild spongiosis) and focal parakeratosis (see Fig E1, A in the Online Repository at www.jacionline.org). Importantly, epidermal disease was more severe on the ear edges (see Fig E1, B). The kinetics of collagen deposition were confirmed by using picrosirius red staining (see Fig E1, C and D). Thus, 4 days of induction with MC903 induced a skin barrier dysfunction with some histopathologic features of AD.[1]

Basophils are the main source of type 2 cytokines in the skin

Unbiased neighboring analysis of leukocyte kinetics measured by high-dimensional spectral flow cytometry from day 0 to day 12 after treatment revealed 12 time-dependent clusters (Fig 2, A). The first cluster contained $CD206^{hi}$ dermal-resident and $MHCII^{hi}$ monocyte–derived $CD64^{hi}$ macrophages, and $CD11b^{+}$, $CD11b^{lo}$ (triple negative, TN) and $CD206^{+}CD301^{+}$ DCs ($CD64^{-}$ $CD11c^{+}$ $MHCII^{+}$). Mast cells (3) ILC2s (7), dendritic epidermal T cells (DETCs), and γδ T cells (5) were identified in the naive skin (day 0). Resident cells were stable over time, with the exception of macrophages and DCs increasing

steadily (Fig 2, A and see Fig E2, A in the Online Repository at www.jacionline.org). The numbers of infiltrating neutrophils (2), Ly6C$^+$ monocytes and macrophages (9), (CD64$^{low/hi}$, respectively), peaked around day 7, whereas eosinophils (10), CD4$^+$ and CD8$^+$ T cells (6), natural killer and natural killer T cells (8) and plasmacytoid DCs (11) peaked at day 10. The numbers of basophils (4), CD4$^-$CD8$^-$ (double-negative) T cells (6), and B cells continued to increase during the resolution phase (Fig 2, B and see Fig E2, B). Cluster 12 represented highly fluorescent CD45$^-$ cells that were excluded from further analyses. These results confirmed the kinetics of the inflammation and resolution phases (Fig 1) and highlighted the disappearance of neutrophils, but not basophils, at the beginning of the resolution phase.

The expression of IL-4 and IL-13 in the skin was mainly restricted to basophils[4] and ILC2s,[7] respectively (Fig 2, C). Only minor subsets of CD4$^+$ T cells were positive for IL-4 or IL-13 (Fig 2, D), contrary to the draining lymph nodes.[27] Basophils were the initial and main source of IL-4 in the skin (Fig 2, C and E and see also Fig E2, C), whereas eosinophils did not show a significant expression of IL-4 or IL-13 (see Fig E2, D). The proportion of IL-13–positive cells was lower than the proportion of IL-4$^+$ cells after day 7 (Fig 2, E). *Il4* gene expression outweighed *Il13* expression by approximately 10-fold to 100-fold from day 9 to day 12 (Fig 2, F). Thus, basophils were the main source of IL-4 in the skin during both inflammation and the resolution.

Cognate CD4$^+$ T cells and eosinophils are redundant for the induction of skin barrier dysfunction

After MC903 treatment, MHCII^{ko} mice[43] showed normal skin inflammation and barrier function (see Fig E3, A in the Online Repository at www.jacionline.org), despite an ablation of CD4$^+$ T cells and an increase of CD8$^+$ T cells and ILC2s in the skin (see Fig E3, B).

Specific conditional depletion of eosinophils[32] impaired the development of skin inflammation but not barrier dysfunction (see Fig E3, C). Eosinophils did not express IL-4 or IL-13 (Fig 2, B and D and see Fig E2, D) or control the expression of IL-4 or IL-13 by basophils, ILC2s, CD4$^+$ T cells, or CD206^{hi} macrophages (see Fig E3, D and E). Overall, neither MHCII-dependent cognate CD4$^+$ T cells nor eosinophils played a nonredundant role in MC903-induced epidermal barrier dysfunction during inflammation.

Basophils are activated both systemically and locally in the skin

Epidermal barrier dysfunction is critical for AD disease[1]; it appeared between day 5 and day 7 (Fig 1, A). From day 4, peripheral blood and BM basophils were more activated: they were bigger and they overexpressed CD11b, FcεRIα, and IL-4. This systemic activation disappeared before day 15 in the BM (see Fig E4, A and B in the Online Repository at www.jacionline.org). Prostaglandin D_2 (PGD_2) mediates eosinophil recruitment and AD-like pathology in a chronic MC903 model,[38] and can activate basophils systemically *in vivo*.[40] In this acute model, however, basophil activation and IL-4/IL-13 expression were not inhibited by AM156 (a CRTH2 [PGD_2 receptor] antagonist) in the spleen or the BM (see Fig E4, C–E). TSLP is a major driver of MC903 induced AD, which was found at day 4 in the serum in this model.[27,28] TSLP is known to activate murine basophils.[2] MC903 did not induce basophil activation at day 4 in TSLPR^{ko} mice (see Fig E4, F). Additionally, FACS-sorted

TSLPR^{ko} basophils injected intradermally in MC903-treated ears did not induce an optimal skin leukocyte recruitment (see Fig E4, G).

TSLP and Cyp24a1 are expressed via a direct response of keratinocytes to MC903, which ceases after treatment. *Cyp24a1* codes for a member of the cytochrome P450 family involved in vitamin D metabolism.[27,28] IL-3 is the most potent cytokine that can activate basophils in the skin.[8] Interestingly, the expression of *Cyp24a1*, a gene known to be induced by TSLP in the MC903 model, decreased from day 7, and from day 9 IL-3 expression was dominant over TSLP, which was not detected anymore (see Fig E4, H).

To explore skin and systemic basophil activation we sort-purified basophils from the spleen and the skin at day 4 or day 15 after MC903 treatment. Spleen basophils showed an increased expression of IL-4, IL-13, and IL-33R at day 4 (but not at day 15). At day 4, skin basophils had a distinct phenotype and expressed more GATA3, IL-6, and amphiregulin but less CCR3. A similar pattern was observed at day 15 (see Fig E4, I and J). Therefore, basophils seemed initially systemically activated by TSLP (days 4–7), but their activation was imprinted by local signals in the skin, which may include IL-3, during both the inflammation and resolution phases (days 7–15).

Basophil and IL-4 control epidermal function and differentiation

Basophil conditional depletion[30] or IL-4 deletion did not reduce ear swelling but delayed and reduced the epidermal barrier dysfunction, which is critical to AD pathogenesis (Fig 3, A).[1] Basophil depletion reduced *Il4* gene expression by approximately 95% (Fig 3, B and C), confirming that basophils are the main source of IL-4 in this model (Fig 2) and suggesting that basophil-derived IL-4 was important for the development of skin barrier dysfunction.

Skin barrier function is tightly controlled by keratinocyte proliferation, differentiation, and cornification.[1,5] Basophils and IL-4 induced epidermal hyperplasia (Fig 3, D) through an expansion of K10$^+$ and FLG$^+$ differentiated keratinocytes (stratum spinosum and stratum granulosum) (Fig 3, E). Basophils also increased the number of proliferating Ki67$^+$K14$^+$ keratinocytes, the area of the K14$^+$ stratum basale (Fig 3, F), and overall keratinocyte differentiation (Fig 3, G).

These results suggested that basophils and IL-4, among other mediators, can promote keratinocyte differentiation, epidermal hyperplasia and skin barrier dysfunction, and cornerstone features of AD.[1] Basophil also promoted the differentiation of keratinocytes expressing the probarrier genes *Flg* and *Dsg1a*.[44,45]

Basophils and IL-4 promote a proresolution leukocyte landscape during inflammation

At day 9 after MC903 treatment, during inflammation, we analyzed skin leukocytes after basophil depletion by performing unbiased neighboring analyses and observed 11 different clusters (Fig 4, A).[41] Specific basophil conditional depletion tended to decrease mast cells and CD206^{hi} and MHCII^{hi} macrophage proportions (Fig 4, B and E), but it increased proinflammatory cells such as neutrophils, CD4$^+$ and CD8$^+$ T cells (Fig 4, C), and Ly6C$^+$ macrophages (Fig 4, D). CD206^{hi} macrophages expressed IL-4 at day 9, and this proportion

decreased after basophil depletion (Fig 4, F).[21,25,46–48] Basophils were also associated with a decrease in ILC2 IL-13 expression (Fig 4, G).[10]

Expression of the M2-associated markers Relmα (*Retlna*) and arginase 1 (*Arg1*) increased from the inflammation phase (day 7) to the resolution phase (day 12) in the skin. Basophil depletion and IL-4 deletion dampened the expression of *Retlna* but not *Arg1* (Fig 4, H). Basophil depletion tended to decrease skin *Alox5* expression, but not expression of *Alox8*, *Alox12*, and *Alox15*, the main specialized proresolution mediators generating lipoxygenases.[49] The expression of the genes coding for IL-3, IL-5, IL-6, and IL-33, but not other type 2–associated signals (IL-10, IL-18, TGF-β, amphiregulin, CCL17, macrophage colony-stimulating factor [M-CSF], galectin 3, and galectin 9) also decreased after basophil depletion. Regulatory T cells (Tregs) did not seem important in the resolution, as *Foxp3* expression decreased from day 0 to day 12 (see Fig E5, A in the Online Repository at www.jacionline.org). Dermal macrophages seemed specifically biased by basophils to express more of the proresolution markers *Alox15* and *Retlna* at day 9 (see Fig E5, B).

Overall, basophils and IL-4 limited the accumulation of proinflammatory cells, induced M2-like macrophages, and favored a proresolution landscape during skin inflammation.

Basophils control dermal-resident macrophage efferocytosis

Efferocytosis is a critical step in the resolution. It is mainly carried out by $CD206^{hi}$ dermal-resident macrophages and by IL-4–expressing macrophages; it is induced by IL-4/IL-13 and involves CD206 expression.[22,24,46,48] Indeed, the majority of dsRed-positive apoptotic cells injected into ears treated on day 9 were taken up by $CD206^{hi}$ dermal-resident macrophages (Fig 5, A). Basophil depletion decreased efferocytosis by skin macrophages. This was due specifically to a defect in the uptake of apoptotic cells by dermal-resident $CD206^{hi}$ macrophages (Fig 5, B). $TUNEL^{+}$ apoptotic cells were observed not only in the epidermis in the control mice (EtOH) but also in the dermis at day 9 after MC903 treatment. The number of apoptotic cells in the skin eventually decreased during the resolution phase (Fig 5, C).

Thus, whereas apoptotic cells accumulated in the dermis during this AD-like inflammation, basophils promoted the proresolution efferocytosis function of dermal-resident $CD206^{hi}$ macrophages.

Basophils show prohomeostatic properties during the resolution phase

Eosinophils express lipoxygenases and can play a proresolution role.[50] As we failed to deplete skin-infiltrated eosinophils during the resolution phase, we could not explore a role of eosinophils in resolution of MC903-induced skin inflammation (see Fig E6, A–C in the Online Repository at www.jacionline.org).

Basophil depletion during the resolution phase led to a small reduction in TEWL.[30] Unexpectedly, this was associated with an accumulation of neutrophils and $Ly6C^{+}$ monocytes but not eosinophils (Fig 6, A). DETC, ILC2, and mast cell proportions and IL-13 expression by DETCs but not by ILC2s decreased following basophil depletion (Fig 6, B).[10] Type 2 cytokine expression by $CD4^{+}$ T cells was unaffected (data not shown). The proportions of macrophages and $PDL2^{+}$ monocyte–derived M2 macrophages[51] were

unchanged, but proinflammatory Ly6C^{+} macrophages tended to accumulate after basophil depletion. Similarly, macrophage expression of the resolution-associated markers CD206 and IL-4 was decreased[24,25,46,48] (Fig 6, C), as was the expression of *Il4* and *Retnla* in the skin (Fig 6, D). Interestingly *Flg* expression and FLG-positive keratinocyte numbers decreased without any change in dermal or epidermal hyperplasia (Fig 6, E and F). Collagen deposition increased in the dermis, as measured after Masson trichrome staining (Fig 6, G) or picrosirius red staining (data not shown). As dermal macrophages internalize and degrade collagen through CD206, which is induced by IL-4, it is likely that basophils promoted this tissue remodeling through control of M2 expansion and function.[26]

Collectively, basophils induced a M2-like macrophage bias, as well as a decrease of proinflammatory cells during the resolution phase, associated with skin repair and remodeling.

Both IL-4 and basophil-derived M-CSF participate in the resolution

IL-4 neutralization during the inflammatory phase did inhibit IgE secretion as expected (see Fig E7, A in the Online Repository at www.jacionline.org). During the resolution phase, it did not inhibit the generation of IgE anymore (see Fig E7, B), nor did it lead to changes in ear swelling, TEWL (Fig 7, A) or total leukocyte infiltration. However, IL-4 did inhibit the accumulation of neutrophils in the skin during the resolution phase (Fig 7, B).

Basophil depletion during the inflammation phase revealed IL-4–independent effects such as keratinocyte proliferation and the expansion of monocyte-derived macrophages (see Figs E2 and E3). Using a transcriptomic database,[52] we looked for the genes expressed by basophils known to be associated with the induction of M2 macrophages or the resolution of inflammation; we found that lipoxygenases (*Alox5, Alox8, Alox12,* and *Alox15*) and M-CSF (*Csf1*) were potently expressed by peripheral basophils (see Fig E7, C). At day 9 after MC903 treatment, basophils expressed similar or higher levels of proresolution genes as eosinophils or macrophages. In addition to *Il4*, they were specifically strong producers of *Alox8*, *Alox12*, *Areg*, *Csf1*, *Il6,* and *Tgfb1* (see Fig E7, D). Although skin basophil expression of *Il4* and *Il13* evolved in a time-dependent manner, *Csf1* expression stayed high from the time of naive conditions to day 12 (see Fig E7, E). As M-CSF is important for both monocyte/macrophage and resident M2 macrophages and shows prorepair and homeostatic functions,[47,53,54] we generated the Basoph8×CSF1$^{fl/fl}$ mice (CSF1$^{\Delta MCPT8}$),[30,35] in which basophils specifically show a ~90% decrease in *Csf1* expression (see Fig E7, F). Topical application of MC903 induced an exacerbated pathology with increased TEWL and/or ear swelling in these mice (Fig 7, C and D) and an altered content of skin immune cells: they showed fewer MHCII^{hi} and CD206^{hi} macrophages, CD4^{+} T cells, γδ T cells, DETCs, and ILC2s at day 12 after MC903 treatment than did their M-CSF–sufficient littermates. CSF1$^{\Delta MCPT8}$ mice also showed an accumulation of neutrophils in the skin (Fig 7, B).

CD206^{hi} dermal-resident and infiltrating macrophage maintenance and M2 phenotype and function rely on both IL-4 and M-CSF.[24,47,54] Together, these results show that IL-4 and basophil-derived M-CSF control M2 homeostasis in an AD-like pathology. Basophils not only initiate skin barrier dysfunction and control epidermal proliferation and differentiation

after MC903 treatment but also promote M2 macrophage expansion and function during skin inflammation and its resolution.

DISCUSSION

Protective type 2 responses emerge following epithelial injury to expel parasites or noxious substances; thus, type 2 cytokines promote a characteristic tissue phenotype that includes mucus secretion, remodeling, repair, and a return to homeostasis. Inappropriate or excessive type 2 responses can become pathogenic if they are not resolved and lead to chronic itching or fibrosis.[19] An intrinsic defect in the barrier function of the epidermis, which is observed in FLG or desmoglein deficiencies, can lead to excessive type 2 inflammation in the skin and to the development of AD.[1,44,55] The type 2 cytokines IL-4 and/or IL-13 are critical for AD chronic inflammation, as shown by the clinical efficacy of dupilumab, but how type 2 effector cells impair or promote the resolution of AD inflammation has not been studied.[1,4]

The occurrence of AD is associated with industrialization, and environmental factors such as pollutants can lead to chronic skin barrier dysfunction and scratching.[56] Such an innate chronic barrier dysfunction allows allergen entry and development of specific adaptive atopic responses. Indeed, MC903 not only induces a TSLP-dependent AD-like dermatitis in the absence of functional adaptive immunity but also promotes specific allergen sensitization through the skin.[11,12,55] TSLP level has been found to be more elevated in the lesional skin of pediatric cases than in adult cases.[57] Most early mild pediatric cases enter remission in the first years of life and do not show high IgE levels or positive results of skin prick tests to common allergens. Severe cases are more persistent and associated with allergen, commensals, or autoantigen sensitization.[58–60] Thus, TSLP could be an important initiator of allergen sensitization and T-cell responses in infants as it is in mice,[9,27,61] but it seems to become redundant once allergen sensitization is driving the disease. Indeed, tezepelumab (a TSLP-neutralizing antibody) failed to improve moderate-to-severe adult AD over placebo when associated with topical corticosteroids, with most patients showing high total IgE titers (>150 kU/L).[62] Epithelial cell–derived cytokines such as TSLP or IL-33 can trigger IL-4 and IL-13 expression by basophils, mast cells, eosinophils, or ILC2s.[63–65] These mechanisms could be more important for AD initiation during infancy than for skin inflammation in adulthood, when potent specific T cells and IgE responses are already established and dominant.

Here we have characterized a common model of TSLP-dependent dermatitis. Mice developed a self-resolving AD-like disease that is histologically closer to acute AD than to adult chronic AD. Allergens were not added with MC903 treatment[12,66] to study more specifically the mechanisms leading to barrier dysfunction before any allergen sensitization could arise. In this regard, this model differed from human AD, which is strongly associated with specific $CD4^+$ T-cell responses. In the study herein we did not observe an MHCII-dependent skin phenotype despite a lymph node expansion of T_H2/T_H13 cells.[27] $CD4^+$ cells were also redundant to induce skin inflammation in a chronic model of MC903-induced AD. Importantly, in the chronic model, skin barrier function was determined by eosinophils and PGD_2,[38] which differs from the acute situation described here. Another limitation of this study is that the remission of human AD inflammation is usually controlled by weeks of

corticosteroid treatment, whereas we studied a model showing spontaneous resolution after removal of the chemical offending the skin.

Immune cell recruitment to the inflamed skin tracked closely with keratinocyte differentiation and skin pathology kinetics. Contrary to proinflammatory cells, IL-4–producing basophils remained in the skin during the resolution phase. Basophils were activated systemically during the initiation of the disease, and they were recruited to the dermis to promote keratinocyte proliferation and differentiation, as well as to accelerate a skin barrier dysfunction in a partially IL-4–dependent manner. However, their role could not be described as completely proinflammatory or pathogenic, as they also promoted the expansion and function of M2-like macrophages, as well as the expression of probarrier genes such as *Flg* and *Dsg1a*, during the inflammation phase. During the resolution phase, basophils supported a proresolution macrophage phenotype, a decrease in proinflammatory cells, epidermal repair, and tissue remodeling. This late support seemed to rely on basophil IL-4 and M-CSF expression. Both proinflammatory and proresolution roles have been attributed to basophils during IgE-mediated chronic and prurigo-like skin inflammation.[16,18] However, in a model of liver infection dominated by type 1 inflammation, basophils showed only some proresolution properties.[17] Indeed, any basophil prohomeostatic properties seem hidden by the deleterious effects of type 2 inflammation during atopy or allergy.

This homeostatic role of basophils has been associated with resident dermal macrophages in our current study, with monocyte-derived macrophages during IgE-mediated skin inflammation,[16,18] with Kupffer cells during liver infection,[17] and with alveolar macrophages during lung development.[67] If basophils seem specialized to interact with distinct macrophages subsets, they also express numerous ligands able to interact with nonhematopoietic cells.[67] Basophils can induce keratinocyte proliferation and differentiation,[15] but they also control the activation of fibroblasts[68,69] and endothelial cells[70] via their secretion of IL-4 and histamine. As IL-4 has been shown to decrease keratinocyte differentiation and Flg expression *in vitro*, it is likely that basophils and IL-4 promoted keratinocyte differentiation and Flg expression through indirect effects in the current model *in vivo* (eg, as a counterbalancing response to increased scratching). Further investigation is needed to understand whether basophils can directly contribute to tissue remodeling and repair.

Cardinal immunologic features of AD include an expansion of T_H2 cells, eosinophils, and ILC2s in the skin, all of which have been observed in various MC903-induced AD-like models.[10,27,71] Surprisingly, eosinophils or cognate T cells did not represent a major source of IL-4/13 in the current model. Hence, our data support the notion that basophil type 2 cytokine production can initiate an innate AD-like pathology.

Thus, basophils can promote a pleiotropic type 2 program inducing both a detrimental skin barrier dysfunction and beneficial efferocytosis, repair, and remodeling through their control of keratinocyte and dermal macrophage functional phenotypes.

Supplementary Material

Refer to Web version on PubMed Central for supplementary material.

Acknowledgments

Funded by an independent research organization grant from the Health Research Council of New Zealand and by the Marjorie Barclay Trust (to G.L.G.), as well as by the National Institutes of Health (grant AG045040) and Welch Foundation (grant AQ-1507 [to J.X.J.]).

We wish to thank the staff of the Malaghan Institute of Medical Research Hugh Green Cytometry Centre, Research Information Technologies and Biomedical Research Unit, for their expert support. We want to sincerely thank Dr Warren Leonard, Dr Elizabeth Jacobsen, the Lee Lab, and Dr Horst Bluethmann for the mice strains and Dr Franca Ronchese for the reagents. We are extremely grateful to Professor Graham Ogg and Dr Mei Li for critical discussions.

Abbreviations used

AD	Atopic dermatitis
B8	Basoph8
BM	Bone marrow
DETC	Dendritic epidermal T cell
dsRed	dsRed.T3
EtOH	Ethyl alcohol
FACS	Fluorescence-activated cell sorting
FLG	Filaggrin
ILC2	Type 2 innate lymphoid cell
iDTR	Cre-inducible diphtheria toxin receptor
K10	Keratin 10
K14	Keratin 14
M-CSF	Macrophage colony-stimulating factor
MHCII	MHC class II
NIH	National Institutes of Health
PGD_2	Prostaglandin D_2
TEWL	Transepidermal water loss
TSLP	Thymic stromal lymphopoietin

REFERENCES

1. Weidinger S, Beck LA, Bieber T, Kabashima K, Irvine AD. Atopic dermatitis. Nat Rev Dis Primers2018;4:1. [PubMed: 29930242]
2. Siracusa MC, Saenz SA, Hill DA, Kim BS, Headley MB, Doering TA, et al.TSLP promotes interleukin-3-independent basophil haematopoiesis and type 2 inflammation. Nature2011;477:229–33. [PubMed: 21841801]
3. Liew FY, Girard J-P, Turnquist HR. Interleukin-33 in health and disease. Nat Rev Immunol2016;16:676–89. [PubMed: 27640624]
4. Harb H, Chatila TA. Mechanisms of dupilumab. Clin Exp Allergy2020;50:5–14. [PubMed: 31505066]
5. Omori-Miyake M, Yamashita M, Tsunemi Y, Kawashima M, Yagi J. In vitro assessment of IL-4- or IL-13-mediated changes in the structural components of keratinocytes in mice and humans. J Invest Dermatol2014;134: 1342–50. [PubMed: 24280725]
6. Oetjen LK, Mack MR, Feng J, Whelan TM, Niu H, Guo CJ, et al.Sensory neurons co-opt classical immune signaling pathways to mediate chronic itch. Cell2017; 171:217–28.e13. [PubMed: 28890086]
7. Hill DA, Spergel JM. The atopic march. Ann Allergy, Asthma Immunol2018;120: 131–7. [PubMed: 29413336]
8. Karasuyama H, Miyake K, Yoshikawa S, Yamanishi Y. Multifaceted roles of basophils in health and disease. J Allergy Clin Immunol2018;142:370–80. [PubMed: 29247714]
9. Leyva-Castillo JM, Hener P, Michea P, Karasuyama H, Chan S, Soumelis V, et al.Skin thymic stromal lymphopoietin initiates Th2 responses through an orchestrated immune cascade. Nat Commun2013;4:2847. [PubMed: 24284909]
10. Kim BS, Wang K, Siracusa MC, Saenz SA, Brestoff JR, Monticelli LA, et al.Basophils promote innate lymphoid cell responses in inflamed skin. J Immunol2014;193:3717–25. [PubMed: 25156365]
11. Hussain M, Borcard L, Walsh KP, Pena Rodriguez M, Mueller C, Kim BS, et al.Basophil-derived IL-4 promotes epicutaneous antigen sensitization concomitant with the development of food allergy. J Allergy Clin Immunol2018;141:223–34.e5. [PubMed: 28390860]
12. Noti M, Kim BS, Siracusa MC, Rak GD, Kubo M, Moghaddam AE, et al.Exposure to food allergens through inflamed skin promotes intestinal food allergy through the thymic stromal lymphopoietin-basophil axis. J Allergy Clin Immunol2014;133:1390–9.e6. [PubMed: 24560412]
13. Schwartz C, Eberle JU, Hoyler T, Diefenbach A, Lechmann M, Voehringer D. Opposing functions of thymic stromal lymphopoietin-responsive basophils and dendritic cells in a mouse model of atopic dermatitis. J Allergy Clin Immunol2016;138:1443–6.e8. [PubMed: 27372565]
14. Borriello F, Granata F, Marone G. Basophils and skin disorders. J Invest Dermatol2014;134:1202–10. [PubMed: 24499736]
15. Hayes MD, Ward S, Crawford G, Seoane RC, Jackson WD, Kipling D, et al.Inflammation-induced IgE promotes epithelial hyperplasia and tumour growth. Elife2020;9:e51862. [PubMed: 31931959]
16. Hashimoto T, Satoh T, Yokozeki H. Protective role of STAT6 in basophil-dependent prurigo-like allergic skin inflammation. J Immunol2015;194:4631–40. [PubMed: 25862819]
17. Blériot C, Dupuis T, Jouvion G, Eberl G, Disson O, Lecuit M. Liver-resident macrophage necroptosis orchestrates type 1 microbicidal inflammation and type-2-mediated tissue repair during bacterial infection. Immunity2015;42:145–8. [PubMed: 25577440]
18. Egawa M, Mukai K, Yoshikawa S, Iki M, Mukaida N, Kawano Y, et al.Inflammatory monocytes recruited to allergic skin acquire an anti-inflammatory M2 phenotype via basophil-derived interleukin-4. Immunity2013;38:570–80. [PubMed: 23434060]
19. Gieseck RL, Wilson MS, Wynn TA. Type 2 immunity in tissue repair and fibrosis. Nat Rev Immunol2018;18:62–76. [PubMed: 28853443]
20. Wynn TA, Vannella KM. Macrophages in tissue repair, regeneration, and fibrosis. Immunity2016;44:450–62. [PubMed: 26982353]

21. Proto JD, Doran AC, Gusarova G, Yurdagul A, Sozen E, Subramanian M, et al.Regulatory T cells promote macrophage efferocytosis during inflammation resolution. Immunity2018;49:666–77.e6. [PubMed: 30291029]
22. Bosurgi L, Cao YG, Cabeza-Cabrerizo M, Tucci A, Hughes LD, Kong Y, et al.Macrophage function in tissue repair and remodeling requires IL-4 or IL-13 with apoptotic cells. Science2017;356:1072–6. [PubMed: 28495875]
23. Chakarov S, Lim HY, Tan L, Lim SY, See P, Lum J, et al.Two distinct interstitial macrophage populations coexist across tissues in specific subtissular niches. Science2019;363:eaau0964. [PubMed: 30872492]
24. Lee SH, Charmoy M, Romano A, Paun A, Chaves MM, Cope FO, et al.Mannose receptor high, M2 dermal macrophages mediate nonhealing Leishmania major infection in a Th1 immune environment. J Exp Med2018;215:357–75. [PubMed: 29247046]
25. Lee SJ, Evers S, Roeder D, Parlow AF, Risteli J, Risteli L, et al.Mannose receptor-mediated regulation of serum glycoprotein homeostasis. Science2002; 295:1898–901. [PubMed: 11884756]
26. Madsen DH, Leonard D, Masedunskas A, Moyer A, urgensen HJ, Peters DE, et al.M2-like macrophages are responsible for collagen degradation through a mannose receptor-mediated pathway. J Cell Biol2013;202:951. [PubMed: 24019537]
27. Ochiai S, Jagot F, Kyle RL, Hyde E, White RF, Prout M, et al.Thymic stromal lymphopoietin drives the development of IL-13 1 Th2 cells. Proc Natl Acad Sci2018;115:1033–8. [PubMed: 29339496]
28. Li M, Hener P, Zhang Z, Kato S, Metzger D, Chambon P. Topical vitamin D3 and low-calcemic analogs induce thymic stromal lymphopoietin in mouse keratinocytes and trigger an atopic dermatitis. Proc Natl Acad Sci U S A2006; 103:11736–41. [PubMed: 16880407]
29. Sullivan BM, Liang H-E, Bando JK, Wu D, Cheng LE, McKerrow JK, et al.Genetic analysis of basophil function in vivo. Nat Immunol2011;12:527–35. [PubMed: 21552267]
30. Pellefigues C, Mehta P, Prout MS, Naidoo K, Yumnam B, Chandler J, et al.The Basoph8 mice enable an unbiased detection and a conditional depletion of basophils. Front Immunol2019;10:2143. [PubMed: 31552058]
31. Abram CL, Roberge GL, Hu Y, Lowell CA. Comparative analysis of the efficiency and specificity of myeloid-Cre deleting strains using ROSA-EYFP reporter mice. J Immunol Methods2014;408:89–100. [PubMed: 24857755]
32. Jacobsen EA, Lesuer WE, Willetts L, Zellner KR, Mazzolini K, Antonios N, et al.Eosinophil activities modulate the immune/inflammatory character of allergic respiratory responses in mice. Allergy2014;69:315–27. [PubMed: 24266710]
33. Hu-Li J, Pannetier C, Guo L, Löhning M, Gu H, Watson C, et al.Regulation of expression of IL-4 alleles. Immunity2001;14:1–11. [PubMed: 11163225]
34. Roediger B, Kyle R, Yip KH, Sumaria N, Guy TV, Kim BS, et al.Cutaneous immunosurveillance and regulation of inflammation by group 2 innate lymphoid cells. Nat Immunol2013;14:564–73. [PubMed: 23603794]
35. Harris SE, MacDougall M, Horn D, Woodruff K, Zimmer SN, Rebel VI, et al.Meox2Cre-mediated disruption of CSF-1 leads to osteopetrosis and osteocyte defects. Bone2012;50:42–53. [PubMed: 21958845]
36. Al-Shami A, Spolski R, Kelly J, Fry T, Schwartzberg PL, Pandey A, et al.A role for thymic stromal lymphopoietin in CD4+ T cell development. J Exp Med2004; 200:159–68. [PubMed: 15263024]
37. Köntgen F, Süss G, Stewart C, Steinmetz M, Bluethmann H. Targeted disruption of the MHC class II Aa gene in C57BL/6 mice. Int Immunol1993;5:957–64. [PubMed: 8398989]
38. Naidoo K, Jagot F, van den Elsen L, Pellefigues C, Jones A, Luo H, et al.Eosinophils determine dermal thickening and water loss in a MC903 model of atopic dermatitis. J Invest Dermatol2018;138:2606–16. [PubMed: 29964034]
39. Schmidt AJ, Mayer JU, Wallace PK, Ronchese F, Price KM. Simultaneous polychromatic immunofluorescent staining of tissue sections and consecutive imaging of up to seven parameters by standard confocal microscopy. Curr Protoc Cytom2019;91:e64. [PubMed: 31763771]

40. Pellefigues C, Dema B, Lamri Y, Saidoune F, Chavarot N, Lohéac C, et al.Prostaglandin D2 amplifies lupus disease through basophil accumulation in lymphoid organs. Nat Commun2018;9:725. [PubMed: 29463843]
41. Ferrer-Font L, Pellefigues C, Mayer JU, Small SJ, Jaimes MC, Price KM. Panel design and optimization for high-dimensional immunophenotyping assays using spectral flow cytometry. Curr Protoc Cytom2020;92:1–25.
42. Moll R, Divo M, Langbein L. The human keratins: biology and pathology. Histochem Cell Biol2008;129:705–33. [PubMed: 18461349]
43. Madsen L, Labrecque N, Engberg J, Dierich A, Svejgaard A, Benoist C, et al.Mice lacking all conventional MHC class II genes. Proc Natl Acad Sci U S A1999;96: 10338–43. [PubMed: 10468609]
44. Samuelov L, Sarig O, Harmon RM, Rapaport D, Ishida-Yamamoto A, Isakov O, et al.Desmoglein 1 deficiency results in severe dermatitis, multiple allergies and metabolic wasting. Nat Genet2013;45:1244–8. [PubMed: 23974871]
45. Pellerin L, Henry J, Hsu CY, Balica S, Jean-Decoster C, Méchin MC, et al.Defects of filaggrin-like proteins in both lesional and nonlesional atopic skin. J Allergy Clin Immunol2013;131:1094–102. [PubMed: 23403047]
46. Zeng MY, Pham D, Bagaitkar J, Liu J, Otero K, Shan M, et al.An efferocytosis-induced, IL-4-dependent macrophage-iNKT cell circuit suppresses sterile inflammation and is defective in murine CGD. Blood2013;121(17):3473–83. [PubMed: 23426944]
47. Jenkins SJ, Ruckerl D, Thomas GD, Hewitson JP, Duncan S, Brombacher F, et al.IL-4 directly signals tissue-resident macrophages to proliferate beyond homeostatic levels controlled by CSF-1. J Exp Med2013;210:2477–91. [PubMed: 24101381]
48. A-Gonzalez N, Quintana JA, Garcıa-Silva S, Mazariegos M, Gonzalez de la Aleja A, Nicolas-Ávila JA, et al.Phagocytosis imprints heterogeneity in tissue-resident macrophages. J Exp Med2017;214:1281–96. [PubMed: 28432199]
49. Serhan CN. Pro-resolving lipid mediators are leads for resolution physiology. Nature2014;510:92–101. [PubMed: 24899309]
50. Isobe Y, Kato T, Arita M. Emerging roles of eosinophils and eosinophil-derived lipid mediators in the resolution of inflammation [abstract]. Front Immunol2012;3:270. [PubMed: 22973272]
51. Gundra UM, Girgis NM, Ruckerl D, Jenkins S, Ward LN, Kurtz ZD, et al.Alternatively activated macrophages derived from monocytes and tissue macrophages are phenotypically and functionally distinct. Blood2014;123:e110–22. [PubMed: 24695852]
52. Heng TSP, Painter MW. Immunological Genome Project Consortium. The Immunological Genome Project: networks of gene expression in immune cells. Nat Immunol2008;9:1091–4. [PubMed: 18800157]
53. McQuin C, Goodman A, Chernyshev V, Kamentsky L, Cimini BA, Karhohs KW, et al.CellProfiler 3.0: xext-generation image processing for biology. PLoS Biol2018;16:e2005970. [PubMed: 29969450]
54. Hamilton TA, Zhao C, Pavicic PG, Datta S. Myeloid colony-stimulating factors as regulators of macrophage polarization [abstract]. Front Immunol2014; 5:554. [PubMed: 25484881]
55. Saunders SP, Moran T, Floudas A, Wurlod F, Kaszlikowska A, Salimi M, et al.Spontaneous atopic dermatitis is mediated by innate immunity, with the secondary lung inflammation of the atopic march requiring adaptive immunity. J Allergy Clin Immunol2016;137:482–91. [PubMed: 26299987]
56. Hendricks AJ, Eichenfield LF, Shi VY. The impact of airborne pollution on atopic dermatitis: a literature review. Br J Dermatol2020;183:16–23. [PubMed: 31794065]
57. Brunner PM, Israel A, Zhang N, Leonard A, Wen H-C, Huynh T, et al.Early-onset pediatric atopic dermatitis is characterized by T H 2/T H 17/T H 22-centered inflammation and lipid alterations. J Allergy Clin Immunol2018; 141:2094–106. [PubMed: 29731129]
58. Flohr C, Johansson SG, Wahlgren C-F, Williams H. How atopic is atopic dermatitis?J Allergy Clin Immunol2004;114:150–8. [PubMed: 15241359]

59. Illi S, von Mutius E, Lau S, Nickel R, Grüber C, Niggemann B, et al.The natural course of atopic dermatitis from birth to age 7 years and the association with asthma. J Allergy Clin Immunol2004;113:925–31. [PubMed: 15131576]
60. Pellefigues CIgE Autoreactivity in atopic dermatitis: paving the road for autoimmune diseases? Antibodies202098;9:47.
61. Leyva-Castillo JM, Hener P, Jiang H, Li M. TSLP produced by keratinocytes promotes allergen sensitization through skin and thereby triggers atopic march in mice. J Invest Dermatol2013;133:154–63. [PubMed: 22832486]
62. Simpson EL, Parnes JR, She D, Crouch S, Rees W, Mo M, et al.Tezepelumab, an anti-thymic stromal lymphopoietin monoclonal antibody, in the treatment of moderate to severe atopic dermatitis: a randomized phase 2a clinical trial. J Am Acad Dermatol2019;80:1013–21. [PubMed: 30550828]
63. Voehringer DBasophil modulation by cytokine instruction. Eur J Immunol2012; 42:2544–50. [PubMed: 23042651]
64. Ricardo-Gonzalez RR, Van Dyken SJ, Schneider C, Lee J, Nussbaum JC, Liang HE, et al.Tissue signals imprint ILC2 identity with anticipatory function. Nat Immunol2018;19:1093–9. [PubMed: 30201992]
65. Junttila IS, Watson C, Kummola L, Chen X, Hu-Li J, Guo L, et al.Efficient cytokine-induced IL-13 production by mast cells requires both IL-33 and IL-3. J Allergy Clin Immunol2013;132:704–12.e10. [PubMed: 23683462]
66. Noti M, Wojno EDT, Kim BS, Siracusa MC, Giacomin PR, Nair MG, et al.Thymic stromal lymphopoietin-elicited basophil responses promote eosinophilic esophagitis. Nat Med2013;19:1005–13. [PubMed: 23872715]
67. Cohen M, Giladi A, Gorki A-DD, Solodkin DG, Zada M, Hladik A, et al.Lung single-cell signaling interaction map reveals basophil role in macrophage imprinting. Cell2018;175:1031–44.e18. [PubMed: 30318149]
68. Nakashima C, Otsuka A, Kitoh A, Honda T, Egawa G, Nakajima S, et al.Basophils regulate the recruitment of eosinophils in a murine model of irritant contact dermatitis. J Allergy Clin Immunol2014;134:100–7.e12. [PubMed: 24713170]
69. Schiechl G, Hermann FJ, Rodriguez Gomez M, Kutzi S, Schmidbauer K, Talke Y, et al.Basophils trigger fibroblast activation in cardiac allograft fibrosis development. Am J Transplant2016;16:2574–88. [PubMed: 26932231]
70. Cheng LE, Sullivan BM, Retana LE, Allen CDC, Liang H-E, Locksley RM. IgE-activated basophils regulate eosinophil tissue entry by modulating endothelial function. J Exp Med2015;212:513–24. [PubMed: 25779634]
71. Salimi M, Barlow JL, Saunders SP, Xue L, Gutowska-Owsiak D, Wang X, et al.A role for IL-25 and IL-33-driven type-2 innate lymphoid cells in atopic dermatitis. J Exp Med2013;210:2939–50. [PubMed: 24323357]

Key messages

- Basophils and IL-4 drive skin barrier dysfunction and keratinocyte differentiation.
- Basophils, M-CSF, and/or IL-4 promote M2 expansion, efferocytosis, and resolution during atopic inflammation.

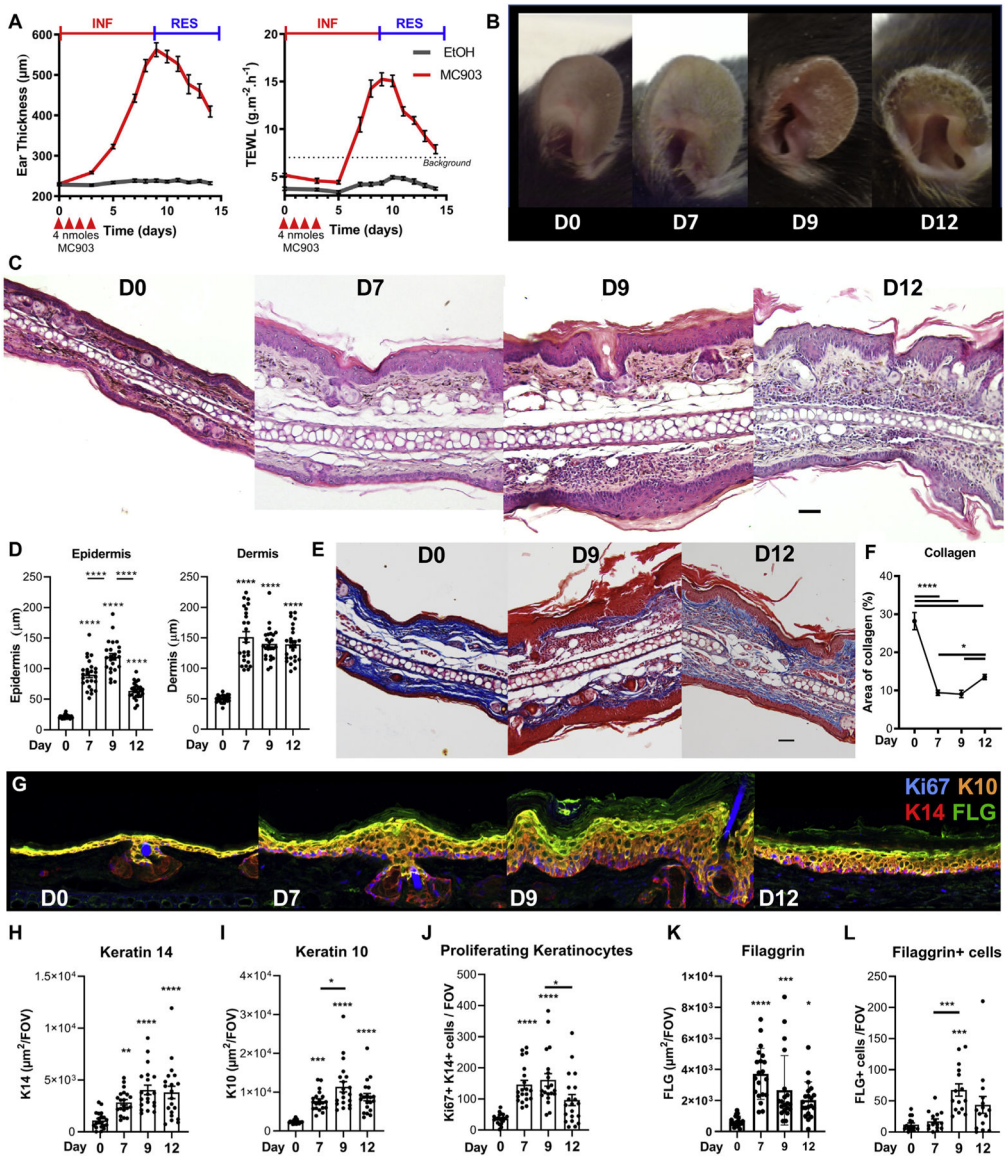

FIG 1.

MC903 induces an AD-like resolving epidermal disease. C57BL/6 mice ears were treated with 4 nmol MC903 or EtOH daily for 4 days. **A,** Ear thickness and TEWL were monitored over time (n = 27). **B,** Representative pictures of the ear skin. **C,** Representative hematoxylin and eosin staining (scale bar = 50 µm; original magnification, ×20). **D,** Quantification of dermal and epidermal thickness (n = 5; 5 fields of view per ear). **E,** Representative Masson trichrome–stained ear tissue sections at day 9 and day 12 (scale bar = 50 µm; original magnification, ×20). **F,** Quantification of the dermal area of collagen (n = 8; 6–8 fields of view per ear; original magnification, ×20). **G,** Representative 3-dimensional reconstruction of Ki67, K14, K10, and FLG immunofluorescent staining of the ear skin (original magnification, ×40). Quantification of the area of K14 (**H**), K10 (**I**), $K14^{+}Ki67^{+}$ keratinocytes (**J**), the area of FLG (**K**), and the number of FLG-positive cells (**L**); **H–K,** n = 4; **L**: n = 3; 5 fields of view per ear. Results are from 5 (**A** and **B**) or 2 (**F–K**) independent

experiments or are representative of at least 2 independent experiments (**C, D,** and **L**). Means ± SEMs are represented. (**D, F,** and **H–L**) Statistics were calculated by using 1-way ANOVA with the Tukey posttest. *$P < .05$; **$P < .01$; ***$P < .001$; ****$P < .0001$. *INF*, Inflammation; *RES*, resolution.

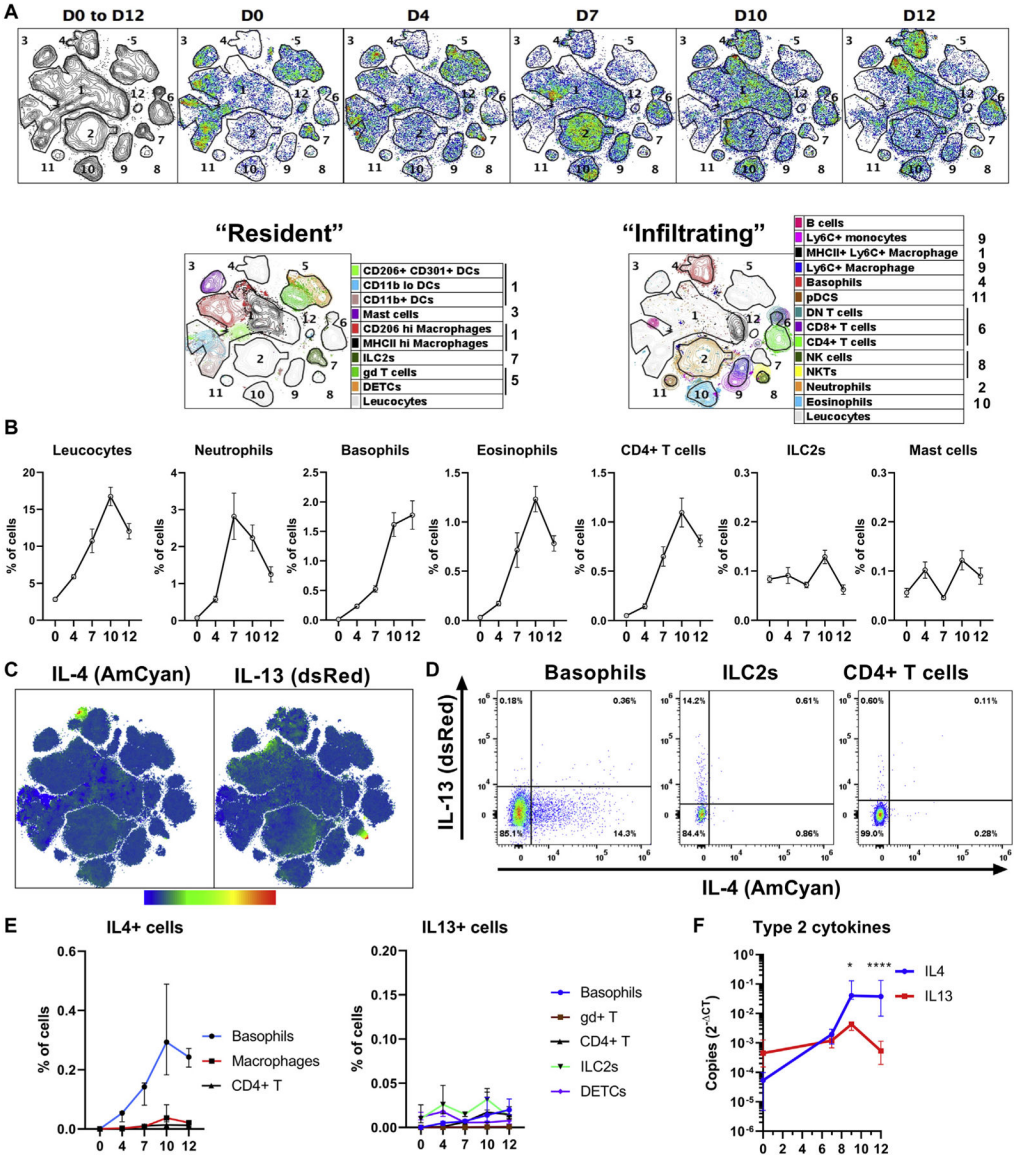

FIG 2.

Basophils are the main source of type 2 cytokines in AD skin. Female B8×4C13R mice were treated with MC903, and their skin leukocytes were analyzed by flow cytometry. **A,** Contour and pseudocolor plots of a representative t-distributed stochastic neighbor embedding analysis of the kinetics of skin leukocyte populations (10,000 $CD45^+$ cells per mouse; 4 mice per day). Clusters were numbered and immune cells were identified in each cluster. **B,** Kinetics of selected leukocytes are depicted (n = 10). **C,** Overall expression of IL-4 (AmCyan) and IL-13 (dsRed) from day 0 to day 12 (as in [**A**]) in heatmap of the intensity of expression. **D,** Representative dot plots showing the expression of IL-4 and IL-13 by basophils, ILC2s, or $CD4^+$ T cells at day 9. **E,** Quantification of the number of IL-4 or IL-13–positive cells (n = 10). **F,** *Il4* and *Il13* transcripts in the ear (n = 4, 5, 5, and 10) over time. Results are representative of at least 2 independent experiments showing similar results. Means ± SEMs (**B**) or medians and interquartile ranges (**E** and **F**)

are represented. **F,** Statistics calculated by using 2-way ANOVA with the Sidak multiple comparison test. *$P < .05$; ****$P < .0001$. *D,* Day.

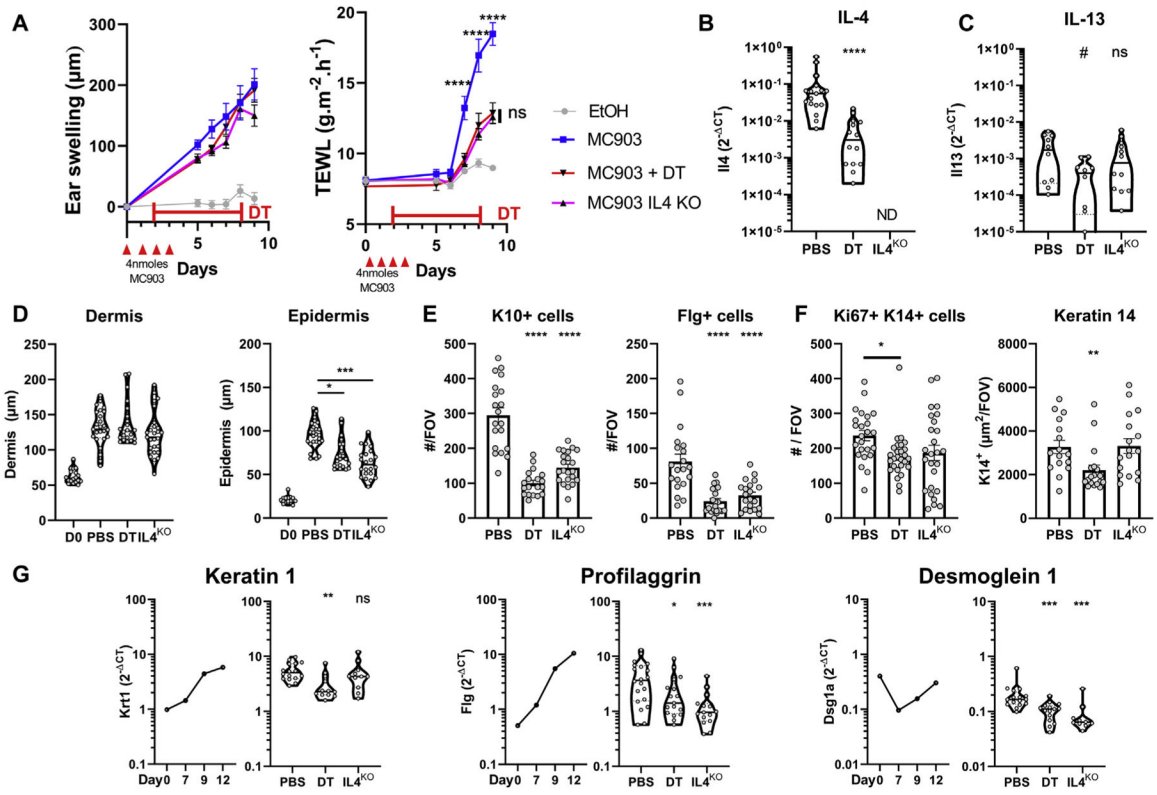

FIG 3.

Basophil-derived IL-4 controls epidermal barrier function and differentiation. B8×iDTR or IL-4^{KO} mice were treated with MC903 or EtOH and diphtheria toxin (DT) or PBS. **A,** Ear swelling and TEWL monitoring (n = 8, 12 , 12, and 14). **B** and **C,** Expression of the genes *Il4* (n = 14 and 17) (**B**) and *Il13* (**C**) in the ear at day 9 (n = 10, 10, and 12). **D,** Dermal and epidermal thickness assessed on hematoxylin and eosin–stained sections (n = 3, 4, 4, and 4; 6 or 7 fields of view per ear) at day 0 or day 9. **E,** Number of K10^{+}, Flg-positive cells assessed at an original magnification of ×40 ((n = 4; 5 or 6 fields of view per ear). **F,** K14^{+}Ki67^{+} cells (n = 5; 5 or 6 fields of view per ear) and K14 area (n = 4; 5 or 6 fields of view per ear) at an original magnification of ×20 at day 9. **G,** C57BL/6 ear gene expression over time (n = 6–10) and at day 9 (n = 10–20). Means ± SEMS (**A, E,** and **F**) or medians and violin plots (**B, C,** and **G**) are represented. Representative of (**A** and **F**) or data from at least 2 independent experiments (**B-E** and **G**). Statistics were calculated by using 2-way ANOVA with a Sidak test (**A**), Kruskall-Wallis test (**D**), or 1-way ANOVA with a Dunnett posttest (**E** and **F**), and Mann-Whitney test (**B, C,** and **G**). *P < .05; **P < .01; ***P < .001; ****P < .0001. *KO,* Knockout; *ND,* not detected; *ns*, nonsignificant.

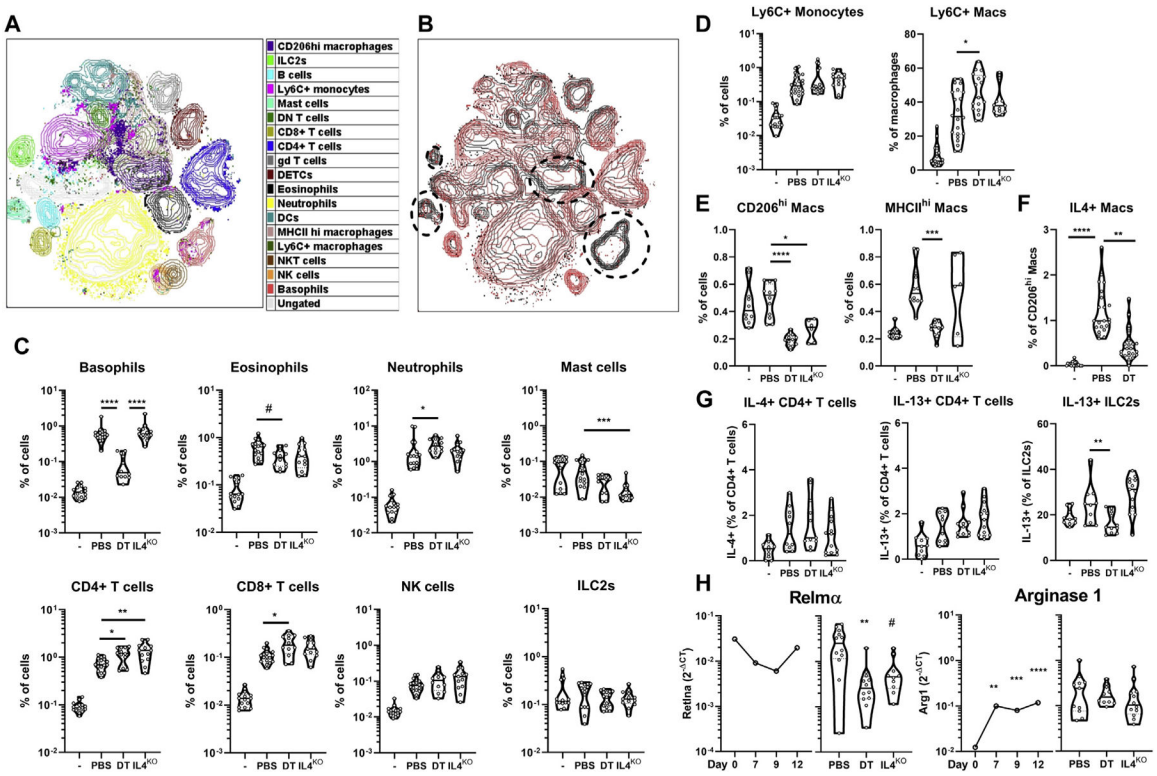

FIG 4.

Basophil-derived IL-4 promotes a proresolution leukocyte landscape during inflammation. B8.4C13RxiDTR mice were treated with MC903 with or without diphtheria toxin (DT) until day 9. Ear $CD45^+$ cells were analyzed by flow cytometry. **A,** Representative t-distributed stochastic neighbor embedding analysis of skin leukocytes populations at day 9 (20,000 $CD45^+$ cells per mouse; n = 5), showing leukocyte clusters. **B,** Overlay of DT treated (*red*) and untreated mice (*black*), revealing depleted clusters. **C,** The proportion of granulocytes and relevant lymphoid cells (n = 13–17), $Ly6C^+$ monocytes or macrophages (n = 13–22) (**D**), $CD206^{hi}$ or $MHCII^{hi}$ macrophages (n = 6–12) (**E**) and the expression of IL-4 (AmCyan) by $CD206^{hi}$ macrophages (n = 19–23) (**F**) or $CD4^+$ T cells or expression of IL-13 (dsRed) by $CD4^+$ T cells and ILC2s (n = 10–13) (**G**) were analyzed at day 9 after EtOH (–) or MC903 treatment without (PBS) or with DT in B8.4C13RxiDTR or IL-4 knockout (KO) ($IL4^{ko}$) mice. **H,** Gene expression of Relm-α and arginase 1 in the whole ear skin was analyzed over time (n = 6–17) and at day 9 (n = 10–12) by quantitative PCR. Medians are represented. Representative of 2 (**A** and **B**) or data from 3 (**C–H**) independent experiments showing similar results. Statistics were calculated by using the Kruskall-Wallis test with a Dunn posttest. #$P < .1$; *$P < .05$; **$P < .01$; ***$P < .001$; ****$P < .0001$. *NK*, Natural killer.

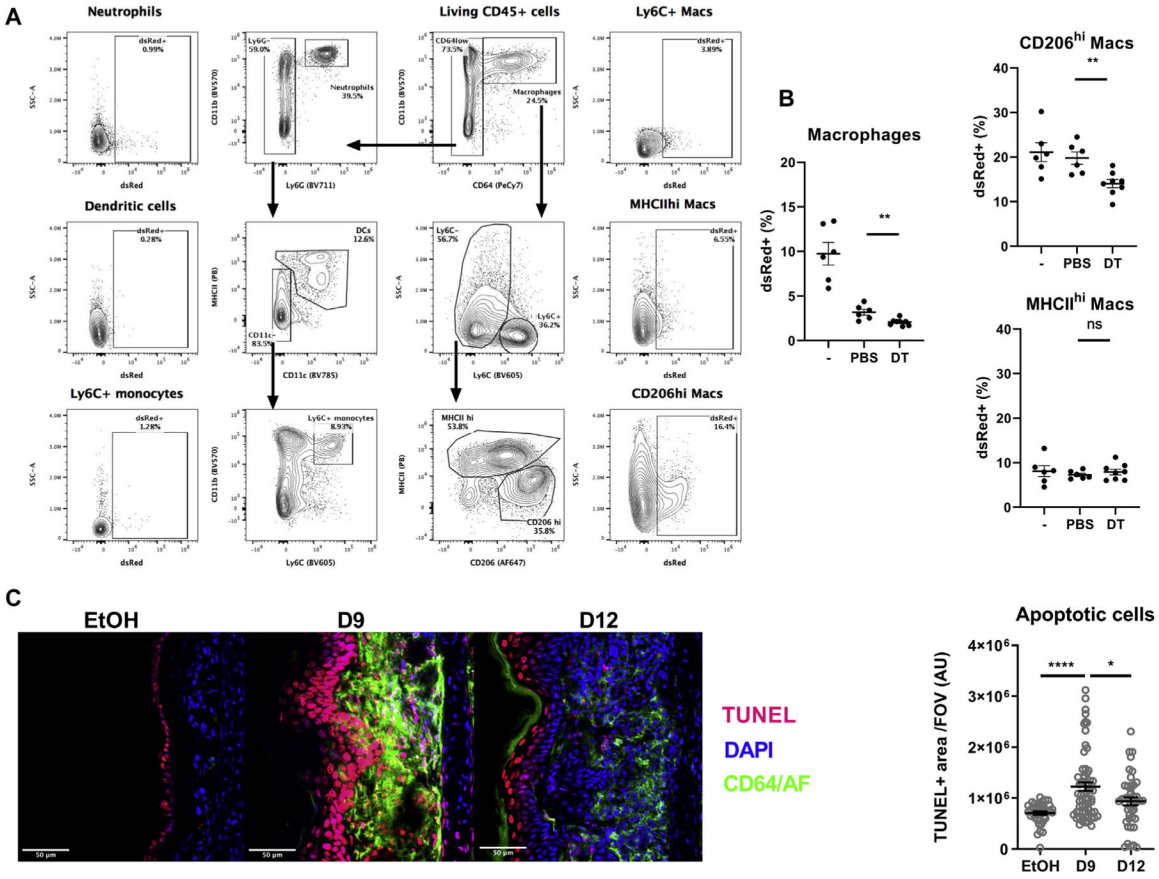

FIG 5.

Basophils control dermal-resident macrophage (Mac) efferocytosis. B8×iDTR mice were treated with EtOH (–) or MC903 for 4 days. The MC903-treated mice were depleted of basophils by injections of diphtheria toxin (DT) or PBS. At day (D) 9 after MC903 treatment, 2M dsRed-postive apoptotic cells were injected in the ear dermis. Two hours later the mice were humanely killed and their ear cells were analyzed by flow cytometry. **A,** Representative gating strategy of skin phagocytes and their uptake of dsRed-positive apoptotic cells. **B,** Histograms representing the efferocytosis of macrophages and relevant subsets as in (**A**) (n = 6–8). **C,** EtOH- or MC903-treated ears were analyzed by immunofluorescence for macrophages and apoptotic cell content was analyzed by TUNEL assay (scale bar = 50 μm). The TUNEL+ area was quantified (n = 5–7 mice with 10 fields of view per mouse). Results are representative of (**A** and **B**) or pooled from (**C**) 2 independent experiments showing similar results. Means ± SEMs are represented. Statistics were calculated by using the unpaired *t* tests. **P* < .05; ***P* <.01; *****P* < .0001. *AF*, Autofluorescence *ns*, nonsignificant.

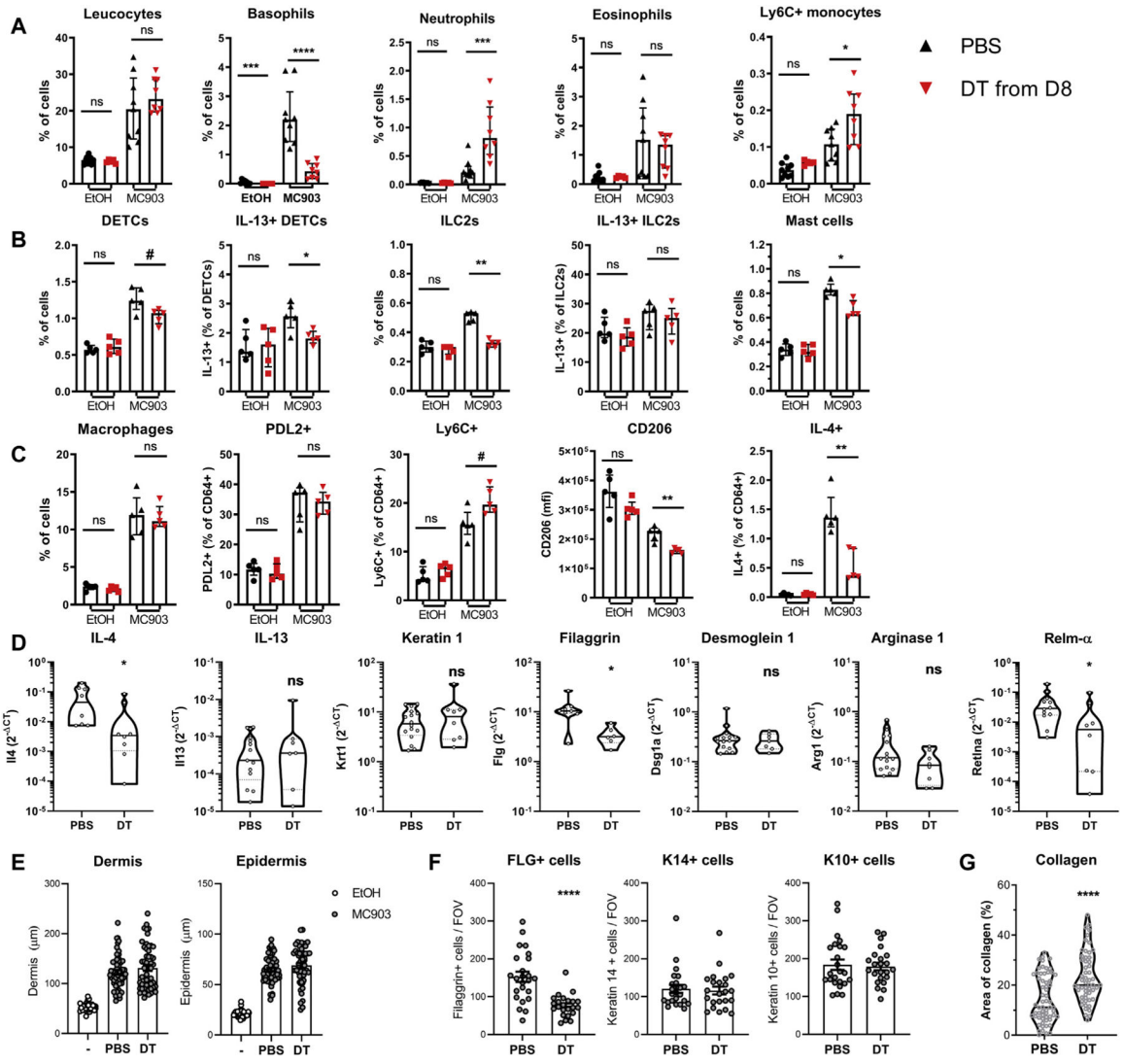

FIG 6.

Basophils show anti-inflammatory and proremodeling properties during the resolution phase. B8.iDTRx4C13R mice were treated with MC903 or EtOH on the contralateral ear and injected with diphtheria toxin (DT) or PBS daily from day 8. At day 12 (**A–C**) ear skin leukocytes were analyzed by flow cytometry (n = 5–9). **D,** Whole skin transcripts of the relevant genes were analyzed by quantitative PCR (n = 8–16). **E,** Dermal and epidermal hyperplasia was quantified on hematoxylin and eosin–stained sections (n = 8 ears with 5–7 sections per ear). **F,** FLG-positive, $K14^+$, and $K10^+$ cells counted from immunofluorescence sections (n = 3 mice; 8 fields of view per ear). **G,** Collagen content was determined on Masson trichrome–stained sections (n = 8 ears with 6 or 7 sections per ear). Results are representative of (**B, C,** and **F**) or pooled from (**A, E,** and **G**) 2 or 3 independent experiments showing similar results. Medians and interquartile ranges (**A–C**), violin plots (**D** and **G**), or means ± SEMs (**E** and **F**) are represented. Statistics were calculated by using Mann-Whitney (**A–D** and **G**) or unpaired *t* tests (**E** and **F**). #$P < .1$; *$P < .05$; **$P < .01$; ***$P < .001$; ****$P < .0001$. *ns*, Nonsignificant.

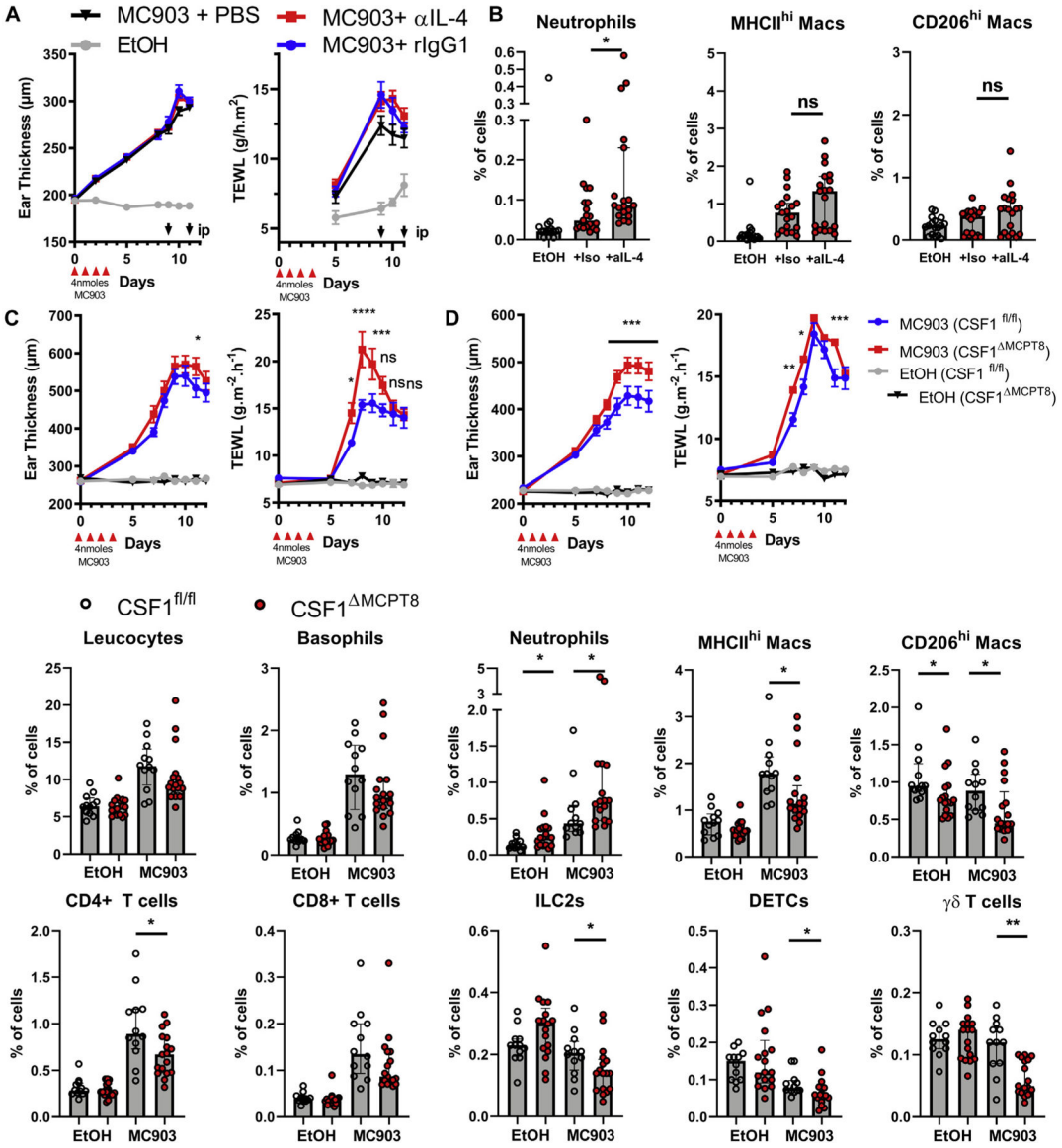

FIG 7.

Basophil-derived IL-4 and M-CSF support the resolution of inflammation. **A,** C57BL/6J were treated with MC903 or EtOH on both ears and injected intraperitoneally with anti–IL-4 (α-IL4), rat IgG1 (iso), or PBS at day 9 and day 11, after which their ear swelling and TEWL were monitored over time (n = 22, 26, 26, and 26) and **B,** their skin leukocytes were analyzed at day 12 by FACS (n = 17, 19, and 19). $B8^{tg/wt}$×$CSF1^{fl/fl}$ ($CSF1^{\Delta MCPT8}$) and $B8^{wt/wt}$×$CSF1^{fl/fl}$ ($CSF1^{fl/fl}$) littermates were treated with MC903 and EtOH on the contralateral ear. **C** and **D,** The ear swelling and TEWL of the males (n = 13 and 16) (**C**) and females (n = 20 and 19 for MC903 and 15 and 9 for EtOH) (**D**) were monitored. **E,** Skin leukocyte populations were quantified by FACS in the female mice at day 12 (n = 12, 12, 17, and 17). Means ± SEMs (**A, C,** and **D**) or medians and interquartile ranges (**B** and **E**) are represented. Statistics were calculated by using 2-way ANOVA with a Tukey posttest comparing each MC903 treated genotype (**A, C,** and **D**) and Mann-Whitney tests (**B** and **E**).

Results are from 2 (**A, B,** and **E**) or 3 (**C** and **D**) independent experiments. *$P < .05$; **$P < .01$; ***$P < .001$; ****$P < .0001$. *MAC*, Macrophage; *ns*, nonsignificant.